

Cobalt(II) Complex of 2,4-Diaminopyrimidine-5-(3,4,5-trimethoxybenzyl)pyrimidine: Experimental and Theoretical Studies

PETER A. AJIBADE

Department of Chemistry, University of Fort Hare, Alice 5700, South Africa

Corresponding author: Fax: +27 86 5181225; Tel: +27 40 6022055; E-mail: pajibade@ufh.ac.za

Received: 16 May 2014;

Accepted: 5 September 2014;

Published online: 4 February 2015;

AJC-16799

Cobalt(II) complex of 2,4-diamino-5-(3',4,5'-trimethoxybenzyl)pyrimidine (trimethoprim) with sulfur ions was synthesized and characterized by elemental analysis, FTIR and electronic spectroscopy. The Co(II) complex formulated as $[\text{Co}(\text{TMP})_2\text{S}_2]$ was confirmed by spectroscopic, single crystal X-ray studies to be in a distorted tetrahedral geometry. The compound contains two molecules of trimethoprim (TMP) and $(\text{S}_2)^{2-}$ dianion. The $(\text{S}_2)^{2-}$ dianion are linked together through non-covalent interactions. Computational analysis confirmed the existence of the dianion in which the each S^- of the $^-\text{S}\cdots\text{S}^-$ dianion is linked together through non covalent interactions and the entire molecule stabilized by hydrogen bond networks. The Co-S bonds in the compound were confirmed through single crystal X-ray and computational studies to be single bonds rather than dithioxocobalt ($\text{Co}=\text{S}$) bonds.

Keywords: Cobalt(II) complex, Spectral studies, Crystal structure, Computational study, Non-covalent interactions.

INTRODUCTION

Compounds containing pyrimidine rings play significant role in many biological systems¹. The pyrimidine ring system provides potential binding sites for metal ions and any information on their coordination properties is important as a means of understanding the role of metal ions in biological systems². Trimethoprim [TMP = 2,4-diamino-5-(3',4,5'-trimethoxy-benzyl)pyrimidine] is a 2,4-diaminopyrimidine derivatives and has seven potential binding sites for metal ions. There have been several studies on the interaction of trimethoprim with metal ions²⁻¹⁵. The initial study based on infrared and electronic spectroscopy measurements inferred the coordination of the metal ions to trimethoprim *via* the NH_2 nitrogen atom³⁻⁵. Other studies⁶⁻¹⁵ based on single crystal X-ray structures of the metal complexes showed that the trimethoprim coordinate the metal ions through the pyrimidinyl N(1) nitrogen atom. Due to the nature of the trimethoprim molecule with several donor atoms, non-covalent interactions play prominent roles in stabilizing its metal complexes.

Non-covalent interactions are of great interest in biology because biomolecules are made by loose aggregate held together by weak interactions¹⁶. Among non-covalent interactions, hydrogen bonding is the most important interaction in molecular recognition because its strength and directional properties plays the most important role in chemistry, biology and material science¹⁷⁻¹⁹. Trimethoprim and other 2,4-diaminopyrimidine

derivatives are antifolate drugs that selectively inhibit the bacterial dihydrofolate reductase enzyme through several hydrogen bonding^{16,20}. In this paper, the synthesis, characterization, single crystal X-ray structure and computational studies of the cobalt(II) complex, $[\text{Co}(\text{TMP})_2\text{S}_2]$ with a disulfide ligand in which the sulfur atoms appear to be independent of each other is reported.

EXPERIMENTAL

All reagents and solvents were of analytical grade and used without further purification. Elemental analysis was carried out on a Perkin-Elmer elemental analyzer. IR spectra of the complex was recorded as KBr pellets on a Perkin-Elmer paragon 2000 FT-IR spectrophotometer in the range 4000-370 cm^{-1} . UV-visible spectrum was recorded using Perkin Elmer 250 UV spectrophotometer in chloroform.

Preparation of the compound: $\text{CoCl}_2 \cdot 6\text{H}_2\text{O}$ (2 mmol, 0.576 g) in absolute methanol (50 mL) was added slowly to a colourless solution of trimethoprim (4 mmol, 1.160 g) in methanol (50 mL). The reaction was refluxed for 2 h and a colourless solution of NH_4NCS (4 mmol 0.304 g) in methanol (25 mL) was added to it and then further refluxed for 2 h. The deep blue solution was filtered and leaves to evaporate slowly at room temperature. Blue crystals suitable for X-ray analysis was obtained after a week. Yield 82 %, Selected IR (KBr, ν_{max} , cm^{-1}): 1666 (C=N), 3335 (N-H)_s, 3472 (N-H)_{as}. Anal. Calcd for $\text{C}_{28}\text{H}_{36}\text{N}_{10}\text{O}_6\text{S}_2\text{Co}$ %: C, 47.66; H, 5.52; N, 18.53; S, 9.09; found: C, 47.46; H, 5.16; N, 18.66; S, 9.04.

Crystal structure determination and refinement: Blue crystals suitable for X-ray analysis were obtained from the reaction mixtures by slow evaporation of the solvent at room temperature. X-ray single crystal intensity data for $[\text{Co}(\text{TMP})_2\text{S}_2]$ was collected on a Nonius Kappa-CCD diffractometer using graphite monochromated MoK_α radiation ($\lambda = 0.71073 \text{ \AA}$). Temperature was controlled by an oxford cryostream cooling system (Oxford Cryostat). The strategy for the data collections were evaluated using the Bruker Nonius "Collect" program. Data were scaled and reduced using DENZO-SMN software²¹. An empirical absorption correction using the program SADABS²² was supplied. The structure was solved by direct methods and refined employing full-matrix least-squares with the program²³ SHELXL-97 refining on F^2 . Packing diagrams were produced using the program PovRay and graphite interface X-seed²⁴. All non-hydrogen atoms were refined anisotropically. The hydrogen atoms on the main molecule were placed in idealized positions in a riding model with U_{iso} set at 1.2 or 1.5 times those of their parent atoms and fixed C-H bond lengths. The structure was refined successfully with final $R = 0.0370$.

Computational methods: The computational simulations were done using FIREFLY 7.1.G²⁵, Gaussian 03²⁶ and AIMAll²⁷ 12.06.03. Natural bond orbital analysis²⁸ have been carried out using NBO 5 G program²⁹ as implemented in FIREFLY 7.1. G which is partially based on the GAMESS (US)³⁰ source code. The charges on each atom were also analyzed on the basis of NPA³¹. All the optimization of the complex and some quantum properties were computed using PBE0 hybrid density functional³² with mixture of two different external basis set obtained from EMSL basis set library^{33,34} which were incorporated into the input file in a format that each FIREFLY and Gaussian programs can read. The complex was initially optimized in FIREFLY using combination of basis set 6-31G which applied valence double zeta (VDZ) and another SBKJC valence double zeta basis set³⁵ with effective core potential (ECP). On atoms of Co and S, SBKJC valence double zeta effective core potential basis set was applied while the remaining atoms were computed using 6-31G basis set. The second optimization was done using G03 with just a little difference of adding polarization to all heavy atoms except H by using 6-31G* basis set. After the optimization, all other computed properties using G03 and FIREFLY were done at this last combination of basis sets. However, some quantum properties were recomputed using computed hybrid functional B3LYP³⁶ and all electron basis set 3-21g³⁷ on the optimized geometries at gas phase of 1 atmosphere and default temperature of 273.15 K in G03 package. The choice of SBKJC valence double zeta effective core potential basis set with PBE0 is as a result of large number of electrons and configurations to be treated and due to the past records of their effectiveness in computational study of metal clusters^{38,39}. The electron density topology and atomic properties were evaluated from the wavefunction computed with B3LYP functional and minimal basis set 3-21 g within quantum theory of atoms in molecules (QTAIM) using AIMAll. The calculation of the atomic properties was carried out by integration within the atomic basins using little modification to the default parameters. In order to present the complementary characteristics of bonds, the topological properties of the

charge density $\rho(r)$ were analyzed using AIM approach to determine both the gradient ($\nabla\rho$) and the Laplacian of the charge density ($\nabla^2\rho$)⁴⁰ as implemented in AIMAll²⁷. In most cases Proaim method of atomic basin integration was used coupled with a very high basin quadrature that correspond to uniform and Gauss-Legendre quadratures for the phi and theta spherical polar angular coordinates respectively. Other parameters used are fine IAS Mesh for adjacent interatomic surface (IAS) paths and Outer Ang of basin quadrature control set to 3/2.

RESULTS AND DISCUSSION

The complex was synthesized by the reaction of a mixture of cobalt(II) chloride, trimethoprim and ammonium thiocyanate in methanol. Slow evaporation of the resulting blue solution over one week afforded copious quantities of blue crystal suitable for structural studies. In forming the complex, the metal ion is coordinated to two molecules of trimethoprim through the pyrimidine N(1) atom and a disulfide ion in which the sulfur atoms appear to be independent of each other. The complex was characterized by elemental analysis, UV-visible, FTIR, single crystal X-ray crystallography and the molecular structure studied by theoretically.

Molecular structure of the compound: The molecular structure of the complex with the atom numbering scheme is shown in Fig. 1. X-ray crystallographic data for the complex are presented in Table-1 and selected bond lengths and angles are given in Table-2. The complex crystallizes in monoclinic space group C2/c in which the Co atom lies on a twofold axis

TABLE-1
SUMMARY OF CRYSTAL DATA AND
STRUCTURE REFINEMENT FOR $[\text{Co}(\text{TMP})_2\text{S}_2]$

Compound	$[\text{Co}(\text{TMP})_2\text{S}_2]$
Empirical formula	$\text{C}_{28}\text{H}_{36}\text{N}_8\text{O}_6\text{S}_2\text{Co}$
Formula weight	703.70
Temperature	173(2) K
Wavelength	0.71073 Å
Crystal system	Monoclinic
Space group	C2/c
Unit cell dimensions	
a (Å)	22.3077(4)
b (Å)	10.3508(3)
c (Å)	15.9331(4)
β (°)	113.796(2)
γ (°)	90
Volume (Å ³)	3366.23(14)
Z	4
D_{calc} Mg/m ³	1.389
Absorption coefficient (mm ⁻¹)	0.686
F(000)	1468
Crystal size (mm)	0.3 × 0.16 × 0.10
Theta range (°)	2.70 to 27.47
Limiting indices	$28 \leq h \leq 28, -13 \leq k \leq 13, -20 \leq l \leq 20$
Reflections collected	111884
Independent reflection	3789 [$R_{\text{int}} = 0.0471$]
Refinement method	Full-matrix least-squares on F^2
Completeness to $\theta = 26.40$	98.4
Data/restraints/parameters/	3789/0/204
Goodness-of-fit on F^2	1.076
Final R indices [$I > 2\sigma(I)$]	$R1 = 0.0370, wR2 = 0.0940$
R indices (all data)	$R1 = 0.0505, wR2 = 0.1031$
Largest diff. Peak and hole e (Å ⁻³)	0.670 and -0.409

TABLE-2
SELECTED BOND LENGTH AND ANGLES FOR [Co(TMP)₂S₂]

Bond length (Å)		Bond angles (°)	
Co(1)-N(3)	2.0256(15)	N(1)#1-Co(1)-N(1)	97.58(9)
Co(1)-N(1)	2.0256(15)	N(1)#1-Co(1)-S(1)#1	107.26(5)
Co(1)-S(1)#1	2.2383(16)	N(1)-Co(1)-S(1)#1	112.07(4)
Co(1)-S(1)	2.2383(6)	N(1)#-Co(1)-S(1)#1	112.07(4)
N(1)-C(1)	1.352(2)	N(1)-Co(1)-S(1)	107.26(5)
N(2)-C(4)	1.355(2)	S(1)#1-Co(1)-S(1)	118.62(5)
N(2)-C(2)	1.340(2)	C(8)-O(1)-C(12)	117.4(2)
N(3)-C(1)	1.343(2)	O(9)-O(2)-C(13)	112.95(16)
N(4)-C(2)	1.344(2)	C(10)-O(3)-C(14)	117.1(2)
O(1)-C(8)	1.369(3)	C(1)-N(1)-C(4)	116.12(15)
O(1)-C(12)	1.420(3)	C(1)-N(1)-Co(1)	130.15(12)
O(2)-C(13)	1.381(2)	C(4)-N(1)-Co(1)	113.71(11)
O(2)-C(14)	1.442(3)	C(2)-N(2)-C(1)	117.63(15)
O(3)-C(10)	1.364(3)	N(3)-C(1)-N(1)	117.17(16)
O(3)-C(14)	1.412(4)	N(2)-C(1)-N(1)	124.54(16)
N(3)-H(4A)	0.8800	N(2)-C(2)-N(4)	117.03(15)

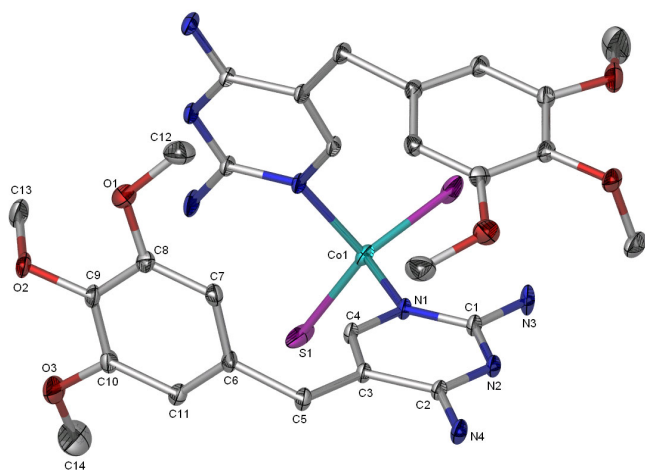


Fig. 1. Molecular structures of [Co(TMP)₂S₂] showing the atomic labeling scheme. All H atoms are omitted for clarity. All non-hydrogen atoms are presented with ellipsoidal model with probability level 25 %

bonding the disulfide ion and two trimethoprim molecules in a distorted tetrahedral environment. The molecular structure of the cobalt complex consists of a discrete molecule, where the central cobalt atom binds to two sulfur atoms of a disulfide ion that appear to be independent of each other and two pyrimidinyl nitrogen atom of each trimethoprim molecule acting as monodentate ligands.

In the molecular structure of the compound, the cobalt atom is tetrahedrally coordinated in CoN₂S₂ form. Thus, the bond angles around the metal center vary from 118.62(5)° for the disulfide ion to 97.58(9)° for the donor atom of the trimethoprim ligands, while the Co-N [2.0256(15)Å] and Co-S [2.2383(16)Å] bond distances are the same. That is, the tetrahedral geometry around the Co(II) atom is distorted with enlargement of the S(1)#1-Co(1)-S(1) [118.62(5)] and a large compression of N(1)#1-Co(1)-N(1) [97.58(9)] with respect to the ideal tetrahedral angles. This may be attributed to the electronegativity of the donor atoms attached to the central Co atom or steric hindrance between the trimethoprim molecules and intramolecular hydrogen bonding interactions (N-H...S) between trimethoprim and the dianion. The distortions in the complex are the results of both the steric repulsion

between the large sulfur atom and the steric hindrances of the trimethoprim molecules. The C-S bond lengths indicate that the bonds are single bonds rather than dithioxocobalt (Co=S) bonds.

The packing diagram of the crystal structure is shown in Fig. 2. In the crystal packing, each discrete molecule of the complex is linked to two other molecules forming parallel chains by intermolecular hydrogen bonding. [Co(TMP)₂S₂] in the crystal lattice consist of parallel chains formed by mutual interactions between molecules through intermolecular H-bonding and each molecule interact with four neighboring molecules. The four intermolecular hydrogen bonds are formed from the oxygen atom from the three methoxy on each trimethoprim molecule and the NH₂. Thus each molecule of trimethoprim acts as H-bond donors as well as acceptors. In this way, each discrete molecule of the complex contains H-bond donors and acceptors. For the intramolecular hydrogen bonding, the NH₂ of the trimethoprim molecule and the disulfide ion are the donors while the acetate oxygen atoms are acceptors. In this way, the packing of the molecule in the crystal lattice comprised of three-dimensional networks consisting of sheets of [Co(TMP)₂S₂] linked by oxygen atoms from the methoxy group.

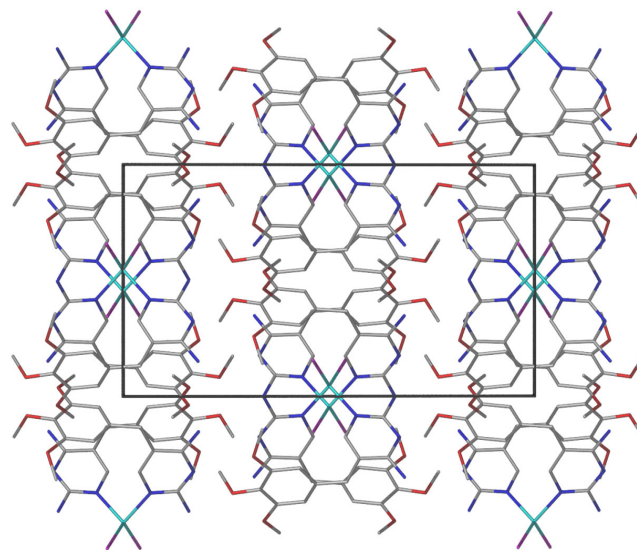


Fig. 2. A packing diagram of [Co(TMP)₂S₂] viewed along [001]. All H atoms are omitted for clarity

Computational studies: The bond distances of all atoms except hydrogen were obtained after the geometry has been optimized are shown in Fig. 3. The feature of the bond order from the computed NPA shows that there is a unique interaction between the two sulfur ions and the H atoms of the neighbouring ligands as shown in Table-3 (S-H* bond with asterisk). The strength of this hydrogen bonds (0.106, 0.166) is very close to the strength of the proposed S-S bond (0.19) as shown in Table-3. The NBO analysis was used to fully understand the electronic communication within the complex and confirm the existence of S-S bond (Table-4). One of the two sulfur atoms is more electronegative than the other with a polarity index of 0.9181 while the other have a polarity index of 0.3964 as shown in Table-4. The results obtained from the second

TABLE-4
NATURAL BOND ORBITALS (NBO) OF THE COMPLEX

Natural bond orbital analysis	Delocalization of electrons from second order perturbation analysis			Natural bond orbital's summary					
	TO	DO	→	TO	AO	E_2	TO	OC	E
(0.91483) BD (1) S1- S2 (84.29 %) 0.9181* S 2 ← (15.71%) 0.3964* S 24	BD (1)	S1-S2	→	LP*(6)	Co	97.14	BD (1)	S1-S2	0.91483-0.17438
(0.99753) BD (1) Co-S1 (23.67 %) 0.4865*Co → (76.33 %) 0.8737* S 2	LP (2)	S1	→	LP*(6)	Co	28.81	BD (1)	Co-S1	0.99753-0.41961
(0.99728) BD (1)Co-S2 (26.01%) 0.5100*Co → (73.99%) 0.8602* S2	LP (2)	S2	→	LP*(6)	Co	29.63	BD (1)	Co-S1	0.99728-0.39629
	LP (3)	S2	→	LP*(6)	Co	96.16			
	LP (1)	N1	→	LP*(6)	Co	41.12			
	LP (1)	N2	→	LP*(6)	Co	42.54			

The orbital analyses in the table are defined in terms of the type of the orbital (TO), donor orbital (DO), acceptor orbital (AO), second perturbation energy or stability energy (E_2 in kcal/mol), occupancy (OC), energy level (E), the term BD(1) means single bond, LP(1) single lone pair while Polarization coefficient c_A is the values with starred superscript in column one.

TABLE-3
BOND ORDER OF THE SELECTED
ATOM-ATOM BOND OF INTEREST IN THE COMPLEX

Bond	Distance	Bond order
Co-S1	2.117	1.360
Co-N	2.055	0.384
Co-S2	2.116	1.396
Co-N	2.052	0.381
S1-S2	3.428	0.192
S1-H*	2.310	0.106
S2-H*	2.311	0.166

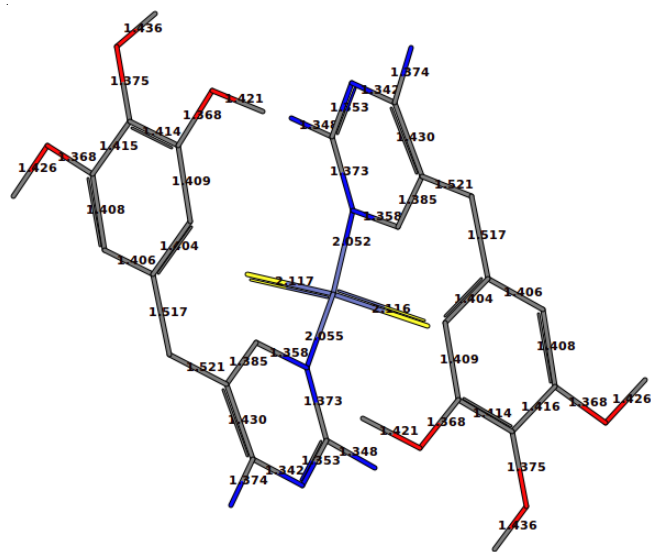


Fig. 3. Computed geometrical distances of the optimized complex

order perturbation theory analysis to estimate the second order energy stability (E_2) clearly show strong ligand to metal charge transfer (LMCT) within the complex.

The feature of the E_2 shows that the ligand-metal interaction are mostly characterized with ligand to metal charge transfer (LMCT). The NBO shows that there is a single bond interaction, BD(1), of S-S bond with occupation value of 0.91483 just as the same BD(1) exist between the two Co-S interaction though with a little higher occupation number than S-S. The results from the NBO analysis show that the energy level of this S-S bond is higher than the two Co-S bonds which is an indication that Co-S is preferred to S-S bond interaction.

Metal complexes are known to possess intense charge transfer transitions⁴¹ and the feature of the HOMO and the LUMO in Fig. 4 shows that the two sulfur atoms dominated

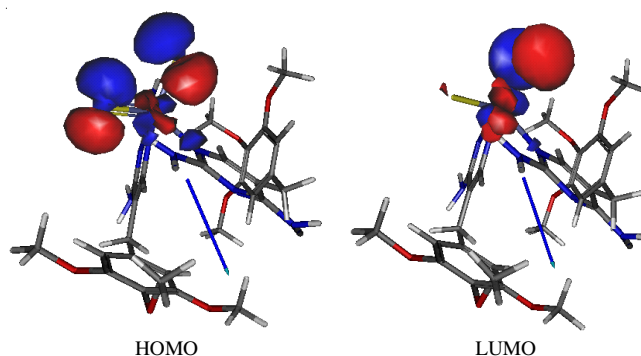


Fig. 4. HOMO (right) and the LUMO (left) of complex with the blue arrow showing the direction of the dipole moment

the HOMO while one of the sulfur and Co atom dominate the LUMO confirming electron transfer from ligand to metal. The reason for the inclusion of one of the sulfur atom as LUMO when it has been suggested to be HOMO initially is traced to the S-S interaction as there is a clear evidence as discussed above that one sulfur is more polarized than the other (Table-4).

The atoms in molecules analysis of the compound using AIMAll confirmed the presence of both strong and weak non-covalent interactions. In interpreting the feature of the quantum theory of atoms in molecules (QTAIM) topology, the critical points density ($\tilde{N}r$) gives information about the existence of bonds, while the sign of Laplacian of the density (\tilde{N}^2r) at that point reflects the kind of interactions such as hydrogen bonds⁴⁰ or ionic or van der Waals bond⁴². The topological features of the electron density from QTAIM analysis using AIMAll shows that the coordination of the two sulfur atoms to the Co atom center were stabilized by the formation of hydrogen bonds with hydrogen atoms of the NH_2 and OCH_3 substituent's on the trimethoprim ligands (Fig. 5). Each of the sulfur atom formed two hydrogen bonds which make the total hydrogen bonds present in the complex up to ten but one from each sulfur atom are the strongest with the Laplacian value ($\tilde{N}^2r(r)$) of 0.067 and 0.069, respectively. Each of the unique hydrogen bonds formed by the two sulfur atom is characterized with ring critical points (red) which are the closest to the metal center among all the ring critical points in the complex. Therefore, the stability of this complex is shown to significantly depend on the complex hydrogen bonds network that exist within the complex and also the presence of the dianion that is coordinated to the metal centre leading to formation of six member ring by the sulfur atoms with substituent's on trimethoprim molecules.

TABLE-5
ELECTRON DENSITY PROPERTIES OF BOND CRITICAL POINT OF SOME SELECTED BONDS OF INTEREST IN THE COMPLEX

Atoms	$r(r)$	\tilde{N}^2r	Ellipticity	K	BPL-GBL_I	V	G	L	GBL_I	V(G)
Co1-S2	9.42×10^{-2}	2.25×10^{-1}	7.16×10^{-2}	3.83×10^{-2}	2.10×10^{-3}	-1.33×10^{-1}	9.45×10^{-2}	-5.62×10^{-2}	4.00	-1.40
Co1-N6	7.75×10^{-2}	3.53×10^{-1}	1.65×10^{-1}	1.81×10^{-2}	3.87×10^{-3}	-1.24×10^{-1}	1.06×10^{-1}	-8.82×10^{-2}	3.88	-1.17
Co1-S24	9.46×10^{-2}	2.22×10^{-1}	3.13×10^{-1}	3.76×10^{-2}	1.06×10^{-2}	-1.31×10^{-1}	9.31×10^{-2}	-5.55×10^{-2}	4.00	-1.40
Co1-N28	7.80×10^{-2}	3.50×10^{-1}	2.00×10^{-2}	1.84×10^{-2}	3.30×10^{-3}	-1.24×10^{-1}	1.06×10^{-1}	-8.75×10^{-2}	3.88	-1.17
S24-H47*	2.42×10^{-2}	6.85×10^{-2}	9.17×10^{-1}	-2.30×10^{-4}	2.80×10^{-3}	-1.67×10^{-2}	1.69×10^{-2}	-1.71×10^{-2}	4.46	-0.99
S2-H65*	2.08×10^{-2}	6.69×10^{-2}	8.10×10^{-2}	-1.15×10^{-3}	8.00×10^{-3}	-1.44×10^{-2}	1.56×10^{-2}	-1.67×10^{-2}	4.46	-0.93
S2-H63	8.92×10^{-4}	2.62×10^{-3}	4.96×10^{-2}	-1.78×10^{-4}	1.10×10^{-2}	-2.98×10^{-4}	4.76×10^{-4}	-6.55×10^{-4}	7.72	-0.63
S24-H81	6.64×10^{-4}	2.10×10^{-3}	4.14×10^{-2}	-1.45×10^{-4}	1.32×10^{-2}	-2.36×10^{-4}	3.81×10^{-4}	-5.26×10^{-4}	7.82	-0.62

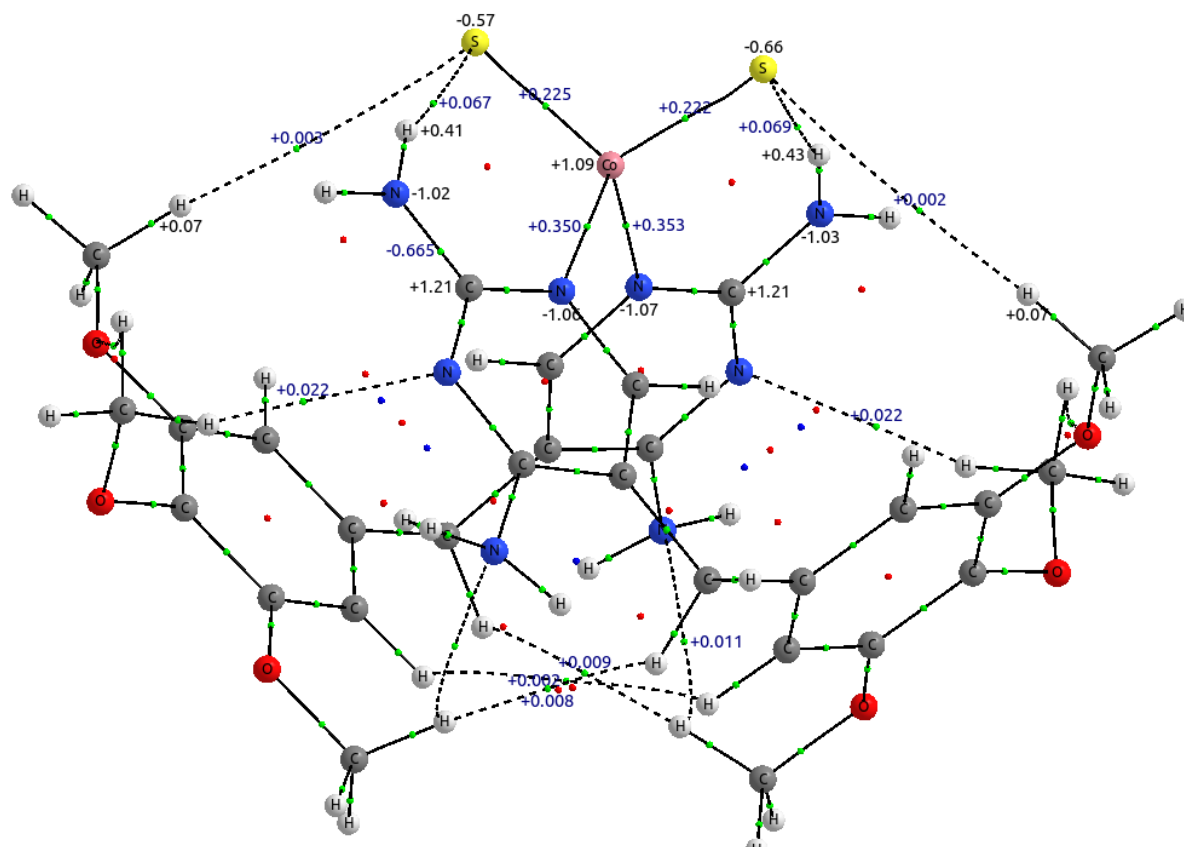


Fig. 5. Intramolecular features in the QTAIM topology of the electron density for complex. (3,-1) bond critical points are shown as small green spheres, (3,+1) ring critical points as small red spheres and (3,+3) cage critical points as small blue spheres

The high positive \tilde{N}^2r values of the metal-ligand bond critical points and corresponding high values of $r(r)$ (Table-5) is an indication of strong non-covalent interactions¹⁸ which is different from the higher negative \tilde{N}^2r values of bonds in the compound that are covalent. The S-H bond distances (GBL_I) of these two unique hydrogen bonds are the same (4.46) as shown in Table-5. The ratio of the electronic potential to kinetic (V/G) for the this unique hydrogen bonds are also lower than that of the other existing S-H bond which further confirm the relatively non-flat nature of electron density of these bonds. The bond order analyses (Table-3) also confirm the existence of this unique hydrogen bonds of the dianion in the complex.

The atomic properties of some of the selected atoms of interest with direct bond to the Co metal are shown in Table-6. All the atomic basins have integrated Laplacian values $L(A)$ of approximately equals to zero (Table-6), indicating satisfactory numerical integration⁴³. The two sulfur atoms are characterized

with the highest volume of the electron density using the isosurface of 0.001 (Table-6) that indicate they both have wide field of interactions responsible for the suggested S-S bond proposed from the NBO analysis (Table-4). The suggested S1-S2 bond from NBO analysis should be relatively weak interaction as it is not recognized in the QTAIM analysis and also the bond order obtained from NPA analysis further confirm that the strength of the S1-S2 bond is just a little higher than the hydrogen bonds (Table-3). These sulfur atoms are also characterized with the highest bonding dipole (Mu_Bond), highest percentage localized electrons [% Loc(A)] and lowest percentage delocalized electrons [% Deloc(A,A')] which indicates that they cannot be easily perturbed by external influences such as an electric field⁴³.

Spectroscopic analysis of the complex: The IR spectra of trimethoprim and the cobalt complex were compared. In the free trimethoprim ligand, the band at 3471 and 3319 cm^{-1}

TABLE-6
SELECTED ATOMIC PROPERTIES DERIVED THROUGH THE QUANTUM
THEORY OF ATOMS IN MOLECULES ANALYSIS FOR THE COMPLEX

Name	q(A)	L(A)	K(A)	K_scaled(A)	lMu_intra(A)	lMu_bond(A)	lMu(A)	N(A)	% Loc(A)	% Delo c(A,A')	Vol (A), 0.001
Co1	1.09	7.84×10^{-4}	1370.02	-1378.51	0.24	0.62	0.46	25.91	93.43	6.57	75.74
S2	-0.57	-6.40×10^{-5}	395.07	-397.52	0.28	1.18	1.26	16.57	94.11	5.89	273.86
S24	-0.66	-5.00×10^{-5}	395.09	-397.54	0.26	1.15	1.28	16.66	94.44	5.56	276.41
N6	-1.07	1.11×10^{-4}	54.51	-54.85	0.29	0.40	0.15	8.07	78.23	21.77	88.14
N28	-1.06	2.06×10^{-4}	54.50	-54.84	0.28	0.40	0.60	8.06	78.15	21.85	87.98
H65*	0.41	6.60×10^{-5}	0.44	-0.44	0.16	0.28	0.42	0.59	24.28	75.72	22.79
H47*	0.43	7.90×10^{-5}	0.42	-0.43	0.16	0.11	0.25	0.57	23.32	76.68	21.83
H63	0.07	5.90×10^{-5}	0.58	-0.58	0.17	0.44	0.60	0.93	42.07	57.93	45.82
H81	0.07	5.80×10^{-5}	0.58	-0.58	0.17	0.58	0.74	0.93	42.21	57.79	45.53

assigned to the symmetrical and asymmetrical N-H stretching frequencies of pyrimidinyl NH₂ shifted in the complex. The broadness of these bands indicate that they are involved in H-bonding^{4,44,45} as confirmed by the single crystal X-ray structure of the complex. This confirms that the NH₂ is not involved in a direct bond formation with the cobalt metal ion. The $\nu(\text{C}=\text{N})$ bands of the pyrimidine N(1) atom which appear as three bands with medium intensities in the ligand occur as a single sharp band, 1670 cm⁻¹ in the complex. The $\nu(\text{CN})$ band of the thiocyanate from NH₄NCS is conspicuously absent in the IR spectrum of the complex as confirmed by the single crystal X-ray structure. The CN might have been eliminated in the course of crystallization of the complex due to steric hindrance. The bands in the region 619-600 cm⁻¹ is assigned to the M-N in the complexes and a broad band at about 480 cm⁻¹ is assigned to the Co-S band of the crystalline sample.

Cobalt(II) is the only common d^7 ion and because of its stereo chemical diversity, its spectra have been widely studied^{46,47}. In a cubic field, three spin allowed transitions are anticipated because of the splitting of the free-ion, ground ⁴F term and the accompanying 4p term. For d^7 ions in tetrahedral crystal fields, the splitting of the free-ion, ground F term is the reverse of that in octahedral field, so that ⁴A_{2g}(F) lies lowest. Thus spectra of a cobalt(II) complexes usually consist of a broad, intense band in the visible region (responsible for the colour and often about 10 times as intense as in octahedral compounds) with a weaker one in the infrared. The electronic spectra of the complex showed two bands at 600 and 650 nm typical of Co(II) tetrahedral complexes.

Conclusion

The mononuclear cobalt(II) complex containing two molecules of trimethoprim and sulfur dianion was synthesized and characterized by elemental analyses, electronic and FTIR spectroscopy. Single crystal X-ray analysis of the compound reveals that the tetrahedral geometry around the cobalt(II) complex consists of two molecules of neutral trimethoprim ligand and sulfur dianion in which the two sulfur atoms are linked by non-covalent interactions. Computational study on the complex revealed that the two sulfur atoms are coordinated to the cobalt ion through a single bond and the compound stabilized by the formation of non-covalent interactions between the sulfur dianion and the NH₂ and OCH₃ of the trimethoprim. NBO analyses further revealed that the strength of the S-S bond is just slightly higher than the hydrogen bonds within the compound.

Supplementary material

CCDC-762860 contains the supplementary crystallographic data for this paper. These data can be obtained free of charge via <http://www.ccdc.cam.ac.uk/conts/retrieving.html>, or from the Cambridge Crystallographic Data Centre, 12 Union Road, Cambridge, CB2 1EZ, UK; fax: (+44)-1223-336-033 or email: deposit@ccdc.cam.ac.uk.

ACKNOWLEDGEMENTS

The contributions of Dr. Hong Su and A.A. Adeniyi and financial support of Govan Mbeki Research and Development centre (GMRDC), University of Fort Hare, South Africa are gracefully acknowledged.

REFERENCES

- N. Saha and S.K.J. Kar, *J. Inorg. Nucl. Chem.*, **39**, 195 (1977).
- E.A. Falco, L.G. Goodwin, G.H. Hitchings, I.M. Rollo and P.B. Russel, *Br. J. Pharmacol.*, **6**, 185 (1951).
- J.J. Burchall, J.W. Corcoran and F.E. Hahn, *Antibiotics*, Springer, New York, Vol. 3, p. 312 (1975).
- P.A. Ajibade, G.A. Kolawole, P. O'Brien and M. Helliwell, *J. Coord. Chem.*, **59**, 1621 (2006).
- P.A. Ajibade, G.A. Kolawole, P. O'Brien, J. Raftery and M. Helliwell, *J. Coord. Chem.*, **61**, 328 (2008).
- L.F. Kuyper, *Computer Aided Drug Design: Methods and Applications*, Marcel Dekker, New York, p. 327 (1989).
- M. Frester, P.M. Furneri, E. Mezzasalma, V.M. Nicolosi and G. Pugeisi, *Antimicrob. Agents Chemother.*, **40**, 2865 (1996).
- B.M. Cooke, N. Mohandas and R.L. Coppel, *Semin. Hematol.*, **41**, 173 (2004).
- D.T.W. Chu, J.J. Plattner and L. Katz, *J. Med. Chem.*, **39**, 3853 (1996).
- J. Verhoef and A. Fluit, *Biochem. Pharmacol.*, **71**, 1036 (2006).
- L. Delhaes, H. Abessolo, L. Berry, P. Delcourt, L. Maciejewski, J. Brocard, D. Camus, D. Dive and C. Biot, *Parasitol. Res.*, **87**, 239 (2001).
- P.A. Ajibade, G.A. Kolawole and P. O'Brien, *Synth. React. Met.-Org. Inorg. Nano-Met. Chem.*, **37**, 653 (2007).
- M. Navarro, F. Vasquez, R.A. Sanchez-Delgado, H. Perez, V. Sinou and J. Schrevel, *J. Med. Chem.*, **47**, 5204 (2004).
- H. Gokhale, S.B. Padhye, S.L. Croft, H.D. Kendrick, W. Davies, C.E. Anson and A.K. Powell, *J. Inorg. Biochem.*, **95**, 249 (2003).
- P.A. Ajibade and G.A. Kolawole, *Transition Met. Chem.*, **33**, 493 (2008).
- N. Stanley, P.T. Muthiah, S.J. Geib, P. Luger, M. Weber and M. Messerschmidt, *Tetrahedron*, **61**, 7201 (2005).
- G.R. Desiraju, *Nature*, **412**, 397 (2001).
- L.J. Prins, D.N. Reinhoudt and P. Timmerman, *Angew. Chem. Int. Ed.*, **40**, 2382 (2001).
- G.R. Desiraju, *J. Mol. Struct.*, **656**, 5 (2003).
- N. Shan, A.D. Bond and W. Jones, *Tetrahedron Lett.*, **43**, 3101 (2002).
- Z. Otwinowski and W. Minor, in eds.: C.W. Carter Jr and R.M. Sweet, *Methods in Enzymology, Macromolecular Crystallography, Part A*, Academic Press, Vol. 276, pp. 307-326 (1997).
- G.M. Sheldrick, SADABS, University of Gottingen, Germany (1996).

23. G.M. Sheldrick, SHELXL-97 and SHELXS-97, University of Gottingen, Germany (1997).
24. L.J. Barbour, *J. Supramol. Chem.*, **1**, 189 (2001).
25. A.A. Granovsky, Firefly, Version 7.1.G, Copyright©1994, Firefly Project, Moscow, Russia (2009); [www.http://classic.chem.msu.su/gran/firefly/index.html](http://classic.chem.msu.su/gran/firefly/index.html).
26. M.J. Frisch, G.W. Trucks, H.B. Schlegel, G.E. Scuseria, M.A. Robb, J.R. Cheeseman, J.A. Montgomery Jr., T.Vreven, K.N. Kudin, J.C. Burant, J.M. Millam, S.S. Iyengar, J. Tomasi, V. Barone, B. Mennucci, M. Cossi, G. Scalmani, N. Rega, G.A. Petersson, H. Nakatsuji, M. Hada, M. Ehara, K. Toyota, R. Fukuda, J. Hasegawa, M. Ishida, T. Nakajima, Y. Honda, O. Kitao, H. Nakai, M. Klene, X. Li, J.E. Knox, H.P. Hratchian, J.B. Cross, C. Adamo, J. Jaramillo, R. Gomperts, R.E. Stratmann, O. Yazyev, A.J. Austin, R. Cammi, C. Pomelli, J.W. Ochterski, P.Y. Ayala, K. Morokuma, G.A. Voth, P. Salvador, J.J. Dannenberg, V.G. Zakrzewski, S. Dapprich, A.D. Daniels, M.C. Strain, O. Farkas, D.K. Malick, A.D. Rabuck, K. Raghavachari, J.B. Foresman, J.V. Ortiz, Q. Cui, A.G. Baboul, S. Clifford, J. Cioslowski, B.B. Stefanov, G. Liu, A. Liashenko, P. Piskorz, I. Komaromi, R.L. Martin, D.J. Fox, T. Keith, M.A. Al-Laham, C.Y. Peng, A. Nanayakkara, M. Challacombe, P.M.W. Gill, B. Johnson, W. Chen, M.W. Wong, C. Gonzalez and J.A. Pople, Gaussian, Inc., Pittsburgh PA (2003).
27. T.A. Keith, AIMAll (Version 12.06.03), TK Gristmill Software, Overland Park KS, USA (2012).
28. J.P. Foster and F.J. Weinhold, *J. Am. Chem. Soc.*, **102**, 7211 (1980).
29. A.E. Reed, L.A. Curtiss and F. Weinhold, *Chem. Rev.*, **88**, 899 (1988).
30. M.W. Schmidt, K.K. Baldridge, J.A. Boatz, S.T. Elbert, M.S. Gordon, J.H. Jensen, S. Koseki, N. Matsunaga, K.A. Nguyen, S. Su, T.L. Windus, M. Dupuis and J.A. Montgomery, *J. Comput. Chem.*, **14**, 1347 (1993).
31. A.E. Reed, R.B. Weinstock and F. Weinhold, *J. Chem. Phys.*, **83**, 735 (1985).
32. C. Adamo and V. Barone, *J. Chem. Phys.*, **110**, 6158 (1999).
33. D.J. Feller, *Comput. Chem.*, **17**, 1571 (1996).
33. K.L. Schuchardt, B.T. Didier, T. Elsethagen, L. Sun, V. Gurumoorthi, J. Chase, J. Li and T.L. Windus, *J. Chem. Inf. Model.*, **47**, 1045 (2007).
34. W.J. Stevens, M. Krauss, H. Basch and P.G. Jasien, *Can. J. Chem.*, **70**, 612 (1992).
36. A.D. Becke, *J. Chem. Phys.*, **98**, 5648 (1993).
37. K.D. Dobbs and W.J. Hehre, *J. Comput. Chem.*, **8**, 861 (1987).
38. B. Marchal, P. Carbonnière, D. Begue and C. Pouchan, *Chem. Phys. Lett.*, **453**, 49 (2008).
39. R. Marchal, P. Carbonnière and C. Pouchan, *Comput. Theoret. Chem.*, **990**, 100 (2012).
40. M.J. Calhorda and P.E.M. Lopes, *J. Organomet. Chem.*, **609**, 53 (2000).
41. P.S. Liyanage, R.M. de Silva and K.M.N. de Silva, *J. Mol. Struct. (Theochem.)*, **639**, 195 (2003).
42. D. Tiana, Ph.D. Thesis, Organometallic Chemistry from the Interacting Quantum Atoms Approach, Università degli Studi di Milano, Milano, pp. 18-19, 46 (2009/2010).
43. J.A. Platts, J. Overgaard, C. Jones, B.B. Iversen and A. Stasch, *J. Phys. Chem. A*, **115**, 194 (2011).
44. B. Simo, L. Perello, R. Ortiz, A. Castineiras, J. Latorre and E. Canton, *J. Inorg. Biochem.*, **81**, 275 (2000).
45. J.M. Tsangaris, D. Sotiropoulos and A.G. Galinos, *Inorg. Nucl. Chem. Lett.*, **14**, 375 (1978).
46. A.B.P. Lever, *Inorganic Electronic Spectroscopy*, Elsevier, Amsterdam, (1984).
47. M.J. Al-Jeboori, A.J. Abdul-Ghani and A.J. Al-Karawi, *Trans. Met. Chem. (Weinh.)*, **33**, 925 (2008).